A Directly Connected OTA Measurement for Performance Evaluation of 5G Adaptive Beamforming Terminals

Penghui Shen, *Student Member, IEEE*, Yihong Qi, *Senior Member, IEEE*, Wei Yu, *Senior Member, IEEE*, Fuhai Li, *Member, IEEE*, Xianbin Wang, *Fellow, IEEE*, and Xuemin Shen, *Fellow, IEEE*

***Abstract*—Spatially beamformed communication, which is achieved by antenna array and multiple-input and multiple-output (MIMO) technologies, has become the most critical technology to drastically increase spectrum utilization rate of 5G. To guarantee the successful deployment of 5G, different aspects of device design, particularly those related to radio-frequency front end and antenna array for enabling beamformed communication, have to be accurately verified. It is more cost effective to identify design imperfections through lab testing rather than using field testing-based trial and error approaches, especially for the explosive growth of 5G-enabled Internet of Things devices. In this article, a directly connected over-the-air (OTA) test solution for 5G MIMO OTA evaluations with the focus on dynamic beamforming devices is proposed. The proposed solution can mathematically achieve constructions among the S ports of base station (BS) and U ports of the receiving antenna array, which makes it possible for measuring the throughput of terminal with an adaptive beamforming array in an OTA way. All system parameters are emulated, including S elements BS antenna gain, U elements of receiving terminal performance, and 3-D $S \times U$ propagation channel characteristics. To further validate the theoretical analysis and test procedure, a newly developed 4 × 4 5G MIMO device is measured in terms of its throughput. The results exactly reflect the true performance of the proposed solution under realistic operational conditions.**

***Index Terms*—5G IoT, adaptive beamforming, directly connected over the air (OTA).**

I. Introduction

SINCE the international standards organization Cellular Telecommunication and Internet Association (CTIA) published the first over-the-air (OTA) measurement standard in 2001 [1], OTA tests have successfully helped the developments of wireless communication from 2G to 5G. In 2020, there are more than 5.2 billion cellular phone users globally [2]. All their performances are required to be measured for passing the OTA network access certifications [3], [4], which also proves that the OTA test has protected the network stability while holding billions of users simultaneously accessed. However, current standard solutions cannot meet the test requirement of 5G multiinput multioutput (MIMO) terminals in the beamforming mode, which is a hindrance for pushing the 5G OTA test standardizations. For solving the issue, an effective solution is proposed in the article and a 4-receiver 5G terminal is used for experimental verifications under a standard 3-dimensional (3-D) channel model.

OTA is a measurement technique for evaluating the wireless performance while maintaining the device under its integrated and normal working mode [5], [6]. The OTA test results can accurately reflect the wireless device's integrated physical link performance of the device under test (DUT). MIMO allows both the transmitting and receiving sides equipped with large numbers of antennas to generate significantly improved throughput through beamformed transmission in a multipath environment [7]–[9]. Similar to 4G MIMO measurements, OTA tests in 5G are also requested to be performed in user equipment (UE) with the multipath channels considered [4], [10], [11]. The key challenge for MIMO performance estimation is how to build a reliable multipath propagation environment in labs, which can emulate the true working scenario of UE in practice [4], [12]–[16].

The CTIA and the 3rd Generation Partnership Project (3GPP) have provided detailed measurement specifications for MIMO [4], [16], where two possible methods for emulating the MIMO multipath propagation environment are specified: 1) the radiated two-stage (RTS) method and 2) the multiple probe anechoic chamber (MPAC) method. The RTS test is achieved based on a first step measurement of the UE antenna pattern actively, which is then combined with the desired multipath channel model in a channel emulator for real-time simulations of the signal propagation environment. The second step of RTS is delivering the simulated signals into the UE receivers for throughput testing [16], [17]. On the other hand, the MPAC method creates the multipath propagations using

Manuscript received 17 February 2021; revised 11 October 2021; accepted 2 February 2022. Date of publication 9 February 2022; date of current version 8 August 2022. This work was supported by the China Postdoctoral Science Foundation under Grant 2021M691679. *(Corresponding author: Yihong Qi.)*

Penghui Shen and Yihong Qi are with the Department of Mathematics and Theory, Peng Cheng Laboratory, Shenzhen 418000, China (e-mail: shenph@pcl.ac.cn; yihong.qi@generaltest.com).

Wei Yu is with the Department of Research and Department, General Test Systems Inc., Shenzhen 418000, China (e-mail: fred.yu@generaltest.com).

Fuhai Li is with the Department of Electrical and Information Engineering, Hunan University, Changsha 410082, China (e-mail: fuhai-li@vip.sina.com).

Xianbin Wang is with the Department of Electrical and Computer Engineering, Western University, London, ON N6A 5B9, Canada (e-mail: xianbin.wang@uwo.ca).

Xuemin Shen is with the Department of Electrical and Computer Engineering, University of Waterloo, Waterloo, ON N2L 3G1, Canada (e-mail: sshen@uwaterloo.ca).

Digital Object Identifier 10.1109/JIOT.2022.3150038

a physical/hardware-enabled approach. Multiple antennas are used to surround the UE for creating the scenario that multiple signals arrive at the UE side simultaneously and in different UE orientations. All measurement antennas are connected to a multichannel channel emulator, where each channel is used for emulating the phase, amplitude, time delay, and Doppler shift varying of the corresponding propagation path in a defined channel model [16], [18], [19].

Both RTS and MPAC methods have been widely used in 4G MIMO testing to improve the overall network performance. However, directly adopting these two standard methods into the 5G UE test may face new challenges. In beamforming working mode, a 5G UE could change its beam dynamically according to the feedback of received parameters [4]. As a consequence, it is almost impossible to obtain the antenna patterns for the traditional RTS approach [4]. The MPAC approach is theoretically feasible. The major challenge, however, comes from the fact that creating a 3-D propagation environment for 5G requires a large number of measurement antennas to surround the DUT, especially for the 5G channel model with more than dozens of clusters coming from different UE directions [4]. In recent years, some significant multiprobe-based schemes have been proposed in order to cope with the OTA test requirements of 5G MIMO terminals and 5G millimeter-wave base stations (BSs), which have brought certain positive contributions to the development of 5G MIMO OTA test standards [22]–[25]. As of now, the standardizations for 5G terminal testing in beamforming mode are still under discussion in 3GPP [26], [27].

To address these issues, a directly connected OTA test solution for 5G MIMO OTA evaluations focusing on dynamic beamforming devices is proposed in this article. The proposed approach first measures the pattern of each DUT antenna unit by a digital signal process (DSP)-enabled algorithm with the DUT transmit/receiver (T/R) module fixed, then simulates the throughput test signal via multiplying the integrated matrix of BS antenna gain, the 3-D channel model, and the measured DUT antenna patterns, and third, delivers the simulated signal to a U port channel emulator side for real-time simulations. Finally, the MIMO throughput test is conducted by building a directly connected OTA link by eliminating cross-couplings among the U ports on the emulator and U ports on the UE antenna units as if the emulator and UE are directly connected.

Compared with the standard RTS method in [17], the proposed directly connected OTA approach is dedicated for $S \times U(S, U >= 2)$ MIMO test based on the following four major improvements. First, a total OTA test solution for 5G MIMO UE in beamforming working mode is proposed in the article, including the constructions of dynamic antenna patterns and the $S \times U$ channel model in computing. Second, for a second-order square matrix in the traditional RTS, it is easy to solve the inverse as long as it is nonsingular. However, for a higher order square matrix, it is better to evaluate its condition order before designing the OTA direct connect process. The higher the condition order, the higher uncertainty contributed by solving the inverse would be brought, and the less stability the throughput measurement would be. Third, 5G MIMO

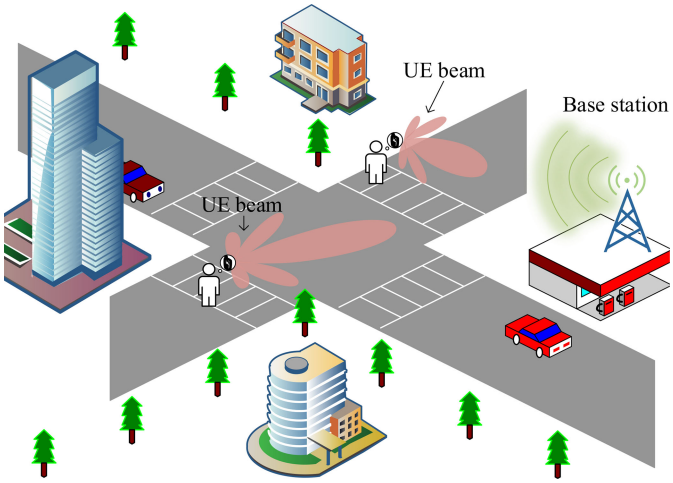

Fig. 1. Schematic illustration for showing the 5G MIMO terminal's real working scenario under dynamic beam-forming mode.

works at a wider bandwidth than 4G, and the propagation matrix in the chamber is frequency selective. So during the OTA direct connect implementations, the channel gain flatness at different frequencies in one band of the RF links (including the measurement antenna gains, the UE antenna gains, and the power loss in chamber) has to be carefully addressed in higher order OTA direct connect establishments. Finally, the 3GPP defined true 3-D channel model has been constructed effectively in chamber for the 5G MIMO OTA test. Prior to this study, 2-D channel models have been used for many years for MIMO performance validations since of some technical limitations. The construction of the 3-D channel model is a key step to promote the standardization of the 5G MIMO OTA test.

The remainder of this article is arranged as follows. The mathematical model of signal propagation in MIMO communication is presented in Section II, followed by the theoretical fundamentals of the proposed directly connected OTA test in Section III. The feasibility of the solution is validated based on a 5G-enabled 4 × 4 MIMO system in Section IV, and finally, the conclusions are drawn in Section V.

II. Mathematical Model of Signal Propagation in MIMO Communications

A. Working Scenario of 5G UE With Adaptive Beamforming

Fig. 1 illustrates how a moving wireless terminal works in a typical working scenario. Since this study is focused on the measurement of 5G UEs, the variation of the terminal beam is highlighted in Fig. 1. In this example, the antenna array of the terminal is steered through signal processing techniques to vary its beam automatically and track the highest signal noise rate (SNR) direction of the BS at all the time.

The practical working scenario can be further depicted as the schematic diagram in Fig. 2. In fact, the electromagnetic signal transmissions for any beamformed communication can be summarized as follows. For the downlink streams, the signals are radiated by the BS antennas, then delivered through the complex propagations channel, and finally, coupled by

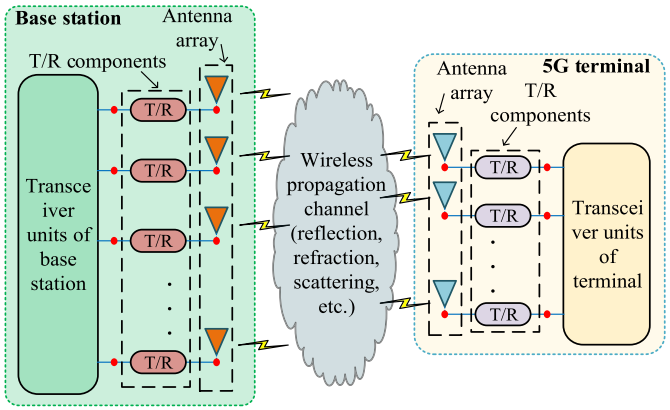

Fig. 2. Schematic diagram of the transmissions between the 5G BS and the mobile wireless terminal.

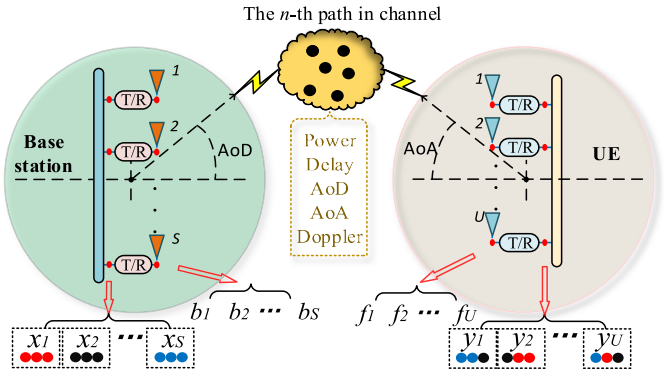

Fig. 3. nth path in channel for MIMO wireless communications.

the mobile terminal antennas, and *vice versa* for the uplink. Thereby, the communication system can be considered as composed of three parts: 1) the BS; 2) the wireless propagation environment; and 3) the mobile UE. Both the BS and UE may consist of a multichannel transceiver and a phased array antenna, which is further composed by a T/R module plus an antenna array.

Generally, the beamforming process uses the T/R module to control the direction of a wave front via appropriately precoding the phase and magnitude of the individual signal in the antenna array. Signals are strengthened at the desired direction by multiple antennas and precoding vectors in order to achieve spatial selectivity. The precoding is processed in baseband based on the estimated channel information from the received signal at the UE side. Hence, the wireless channel (including the characteristics of reflections, refraction, scatterings, Doppler, etc.) plays a dominant role in the beamforming process. In general, the multipath channel can be exploited for capacity augmentation using the MIMO technique. However, the superposition of direct and multiple reflected signal paths could create deep fading. Due to the pros and cons of the multipath effect, evaluating the 5G MIMO DUT's RF performance should take the characteristics of the channel into considerations.

B. Mathematical Model of the Methioned 5G UE Working Scenario

An accurate channel model, which can be validated by experimental results, is critical to quantify practical wireless propagation mathematically. All the influences caused by the surroundings, movements, etc., to signal propagation could be characterized by an ideal channel model, which typically consists of different factors, such as fading statistics, power delay profile, delay spread, cross-polarization rate, Angle of Departure (AoD), Angle of Arrival (AoA), etc. The 3GPP has proposed many standard multipath channel models for wireless DUT performance evaluations [21], [22], where all the transmission paths can be traced mathematically. Fig. 3 shows a typical channel model with N paths, where $(x_1, x_2, \ldots, x_S)$ are the S transmitted signals at the BS transceivers (marked as the BS transmitted signals in the rest), and $(y_1, y_2, \ldots, y_U)$ are the U received signals at the receiver inputs after the UE transceiver components (marked as the UE received signals in the rest). It is clear that after crossing through the N path channel, the received signals become the multiplication of the radiations pattern of BS, the channel model, and the radiation pattern of UE.

Based on the channel model, the UE received signals are associated with the BS transmitted signals as

$$[y_1, y_2, \ldots, y_U]^T = H(t) * [x_1, x_2, \ldots, x_S]^T \tag{1}$$

where

$$H(t) = \sum_{n=1}^{N} \begin{bmatrix} h_{1,1,n}(t) & h_{1,2,n}(t) & \cdots & h_{1,S,n}(t) \\ h_{2,1,n}(t) & h_{2,2,n}(t) & \cdots & h_{2,S,n}(t) \\ \vdots & \vdots & \ddots & \vdots \\ h_{U,1,n}(t) & h_{U,2,n}(t) & \cdots & h_{U,S,n}(t) \end{bmatrix} \tag{2}$$

is the defined channel matrix in MIMO communications, and t denotes time variable. Generally, recovery of the BS transmitted signals can be achieved by on multiplying the UE received signals with the inverse matrix of estimated $H(t)$ at the UE side. The (u, s, n) component of the matrix $H(t)$ is further expressed as [15]

$$h_{u,s,n}(t) = e^{\psi_n} \cdot i_u(t) e^{j\tau_u(t)} \begin{bmatrix} g^v_{u,UE}(\varphi_{n,\mathrm{AoA}}) \\ g^h_{u,UE}(\varphi_{n,\mathrm{AoA}}) \end{bmatrix}^T * \begin{bmatrix} \chi_n^{v,v} & \chi_n^{v,h} \\ \chi_n^{h,v} & \chi_n^{h,h} \end{bmatrix} * \begin{bmatrix} g^v_{s,BS}(\varphi_{n,\mathrm{AoD}}) \\ g^h_{s,BS}(\varphi_{n,\mathrm{AoD}}) \end{bmatrix} p_s(t) e^{j\upsilon_s(t)} \tag{3}$$

where ψ_n is the phase factor including the information about the Doppler effect, phase, and delay of the nth path; $\varphi_{n,\mathrm{AoA}}$, $\varphi_{n,\mathrm{AoD}}$, and $\chi_n^{x,y}$ represent AoA, AoD, and complex amplitude phase change from y to x polarization in the nth path, respectively; $g^x_{u,\mathrm{UE}}(\varphi_{n,\mathrm{AoA}})$ and $g^x_{s,\mathrm{BS}}(\varphi_{n,\mathrm{AoD}})$ are the gain of UE uth antenna plus its corresponding T/R component and the gain of BS sth antenna plus its corresponding T/R component in x polarization separately; $p_s(t)$ and $\upsilon_s(t)$ are the time-varying amplitude and phase gains of the uth T/R element in BS side separately; $i_u(t)$ and $\tau_u(t)$ are the time-varying amplitude and phase gains of the uth T/R component in UE side separately; and $[]^T$ denotes matrix transpose.

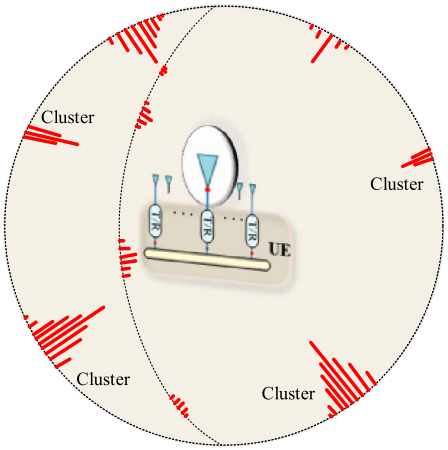

Fig. 4. Diagram of a UE in a 3-D multiple path channel model.

While in the adaptive beamforming working mode, the amplitude and phase offsets of the UE T/R module are controlled by the baseband processing, which are dynamic and unknown to the test system while considering the DUT as a black box. Consequently, the received signals at the UE receivers could not be determined mathematically and emulated in the testing instrument. That is, a major obstacle for the traditional MIMO test standard applying in 5G.

III. Theoretical Foundation of Directly Connected OTA Test Solution

As discussed earlier, the received signals at UE receivers in practice are $(y_1, y_2, \ldots, y_U)$, as defined in (1)–(3). In this article, we focus on producing the signals into UE receivers to emulate the UE's true working condition and evaluate its RF performance. Directly simulating the UE received signals and transferring them to the UE corresponding receivers may be inaccessible, as mentioned before. However, as shown in Fig. 4, for a beamformed MIMO UE in a multipath channel, the signal reaching any UE antenna feeding (before coupling into the UE T/R component) is determined by the BS antennas, multipath channel, and UE antenna unit. The BS antenna patterns and the multipath channel information are known for MIMO test (as specified in [21], [22], and [28]), and the signal reaching any UE antenna feeding is available with the UE antenna unit pattern measured.

So this study will fulfil this objective in two steps: 1) computing the signals $(f_1, f_2, \ldots, f_U)$ at the UE antenna array feedings (marked as the UE antenna feeding signals in the rest), as shown in Fig. 3 and 2) delivering them into the UE antenna unit feedings via directly connected OTA. During testing, ensure the UE in its normal beamforming statements, so that the received signals are equal to $(y_1, y_2, \ldots, y_U)$, which is elaborated as follows.

Here, $(b_1, b_2, \ldots, b_S)$ are the S transmitted signals at the BS antenna element feedings (after passing through the BS T/R components, marked as the BS antenna feeding signals), and $(f_1, f_2, \ldots, f_U)$ are the U received signals at the UE antenna element feedings (before passing the UE T/R components). Then, the UE antenna feeding signals are associated with the UE received signals as

$$\begin{bmatrix} y_1 \\ y_2 \\ \vdots \\ y_U \end{bmatrix} = \begin{bmatrix} i_1(t)e^{j\tau_1(t)} & 0 & \cdots & 0 \\ 0 & i_2(t)e^{j\tau_2(t)} & \cdots & 0 \\ \vdots & \vdots & \ddots & \vdots \\ 0 & 0 & \cdots & i_U(t)e^{j\tau_U(t)} \end{bmatrix} * \begin{bmatrix} f_1 \\ f_2 \\ \vdots \\ f_U \end{bmatrix}. \tag{4}$$

Similar to the above derivations of (4), the BS antenna feeding signals are associated with the BS transmitted signals as

$$\begin{bmatrix} b_1 \\ b \\ \vdots \\ b_S \end{bmatrix} = \begin{bmatrix} p_1(t)e^{j\upsilon_1(t)} & 0 & \cdots & 0 \\ 0 & p_2(t)e^{j\upsilon_2(t)} & \cdots & 0 \\ \vdots & \vdots & \ddots & \vdots \\ 0 & 0 & \cdots & p_S(t)e^{j\upsilon_S(t)} \end{bmatrix} * \begin{bmatrix} x_1 \\ x_2 \\ \vdots \\ x_S \end{bmatrix}. \tag{5}$$

Through (1), (4), and (5), the relationship between the UE antenna feeding signals and the BS antenna feeding signals is

$$[f_1, f_2, \ldots, f_U]^T = \widetilde{H(t)} * [b_1, b_2, \ldots, b_S]^T \tag{6}$$

where $\widetilde{H(t)}$ is expressed as (7), shown at the bottom of the page. Substituting (3) into (7), the (u, s, n) element in matrix $\widetilde{H(t)}$ can be obtained as

$$\frac{h_{u,s,n}(t)}{i_u(t)e^{j\tau_u(t)}p_s(t)e^{j\upsilon_s(t)}} = e^{\psi_n}\begin{bmatrix} g^v_{u,UE}(\varphi_{n,\mathrm{AoA}}) \\ g^h_{u,UE}(\varphi_{n,\mathrm{AoA}}) \end{bmatrix}^T * \begin{bmatrix} \chi_n^{v,v} & \chi_n^{v,h} \\ \chi_n^{h,v} & \chi_n^{h,h} \end{bmatrix} * \begin{bmatrix} g^v_{s,BS}(\varphi_{n,\mathrm{AoD}}) \\ g^h_{s,BS}(\varphi_{n,\mathrm{AoD}}) \end{bmatrix}. \tag{8}$$

Equation (8) denotes that the matrix $\widetilde{H(t)}$ is independent of the T/R units. From (6)–(8), the factors as the BS output streams, beamforming situations, the antenna array pattern at both UE and BS, and the channel model are all consisted in the UE antenna feeding signals, which are further required to be simulated and sent into the UE antenna array feedings without cross-coupling. It is also the next step implemented in this study. Through (6)–(8), the proposed solution mathematically achieves constructions among the S ports of BS and U

$$\widetilde{H(t)} = \sum_{n=1}^{N} \begin{bmatrix} \frac{h_{1,1,n}(t)}{i_1(t)e^{j\tau_1(t)}p_1(t)e^{j\upsilon_1(t)}} & \frac{h_{1,2,n}(t)}{i_1(t)e^{\tau_1(t)}p_2(t)e^{j\upsilon_2(t)}} & \cdots & \frac{h_{1,S,n}(t)}{i_1(t)e^{j\tau_1(t)}p_S(t)e^{j\upsilon_1(t)}} \\ \frac{h_{2,1,n}(t)}{i_2(t)e^{j\tau_2(t)}p_1(t)e^{j\upsilon_1(t)}} & \frac{h_{2,2,n}(t)}{i_2(t)e^{j\tau_2(t)}p_2(t)e^{j\upsilon_2(t)}} & \cdots & \frac{h_{2,S,n}(t)}{i_2(t)e^{j\tau_2(t)}p_S(t)e^{j\upsilon_S(t)}} \\ \vdots & \vdots & \ddots & \vdots \\ \frac{h_{U,1,n}(t)}{i_U(t)e^{j\tau_U(t)}p_1(t)e^{j\upsilon_1(t)}} & \frac{h_{U,2,n}(t)}{i_U(t)e^{j\tau_U(t)}p_2(t)e^{j\upsilon_2(t)}} & \cdots & \frac{h_{U,S,n}(t)}{i_U(t)e^{j\tau_U(t)}p_S(t)e^{j\upsilon_S(t)}} \end{bmatrix} \tag{7}$$

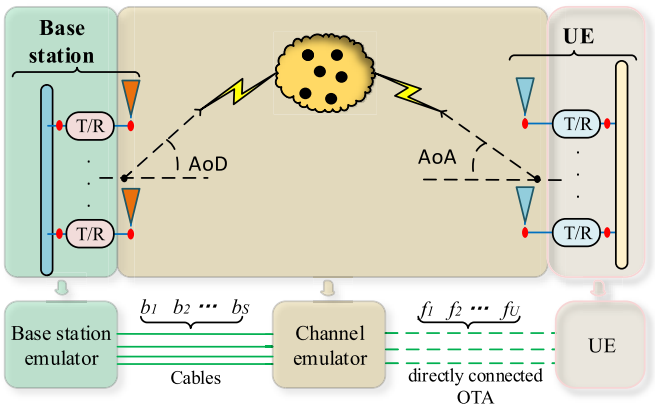

Fig. 5. Implementations of the proposed solution.

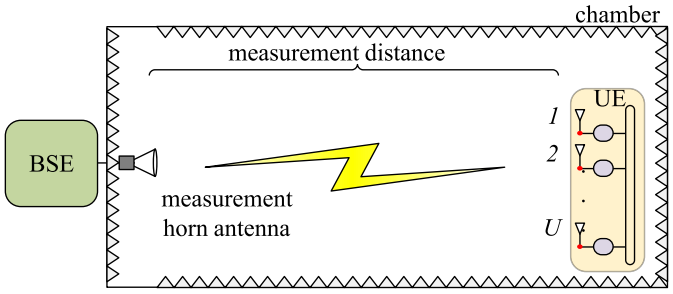

Fig. 6. Simplified test setting for the UE antenna element pattern measurements.

ports of UE receivers, which makes it possible for measuring throughput of terminal with adaptive beamforming array in an OTA way, as discussed as follows.

A. Calculations of the UE Antenna Feeding Signals

Since the gains of the antenna elements in both UE and BS are time independent, all the parameters in (6) and (8) are accessible for the matrix $\widetilde{H(t)}$ computing, that is the basic theory foundation of the proposed solution in this article. Combining (1), (4), (5), and (7), we can have that

$$\begin{aligned}\left[y_1, y_2, \ldots, y_U\right]^T &= Ie * \widetilde{H(t)} * Pe * [x_1, x, \ldots, x_S]^T \\ [b_1, b_2, \ldots, b_S]^T &= Pe * [x_1, x, \ldots, x_S]^T \\ \left[f_1, f_2, \ldots, f_U\right]^T &= \widetilde{H(t)} * Pe * [x_1, x, \ldots, x_S]^T \end{aligned} \tag{9}$$

where Ie and Pe are the T/R module excited diagonal matrixes defined in (4) and (5), respectively. Equation (9) details the signal transmissions in practical communications, which is further implemented in the presented test solution in Fig. 5, based on three facts.

First, it is almost impossible to access the factor Ie from a general UE while under testing in beamforming mode. However, for UE tests, a BS emulator (BSE) is required for imitating all the features of a real BS, including generating the test signals, changing the beam automatically, etc. Therefore, the BS antenna feeding signals are known and can be simulated in the BSE.

Second, the patterns of the antenna elements of the BS and channel models are specified by the 3GPP standards. The gains of the antenna elements in UE are accessible through a DSP enabling algorithm inside the UE. In MIMO communication, after receiving the multistream signals, a UE will do the channel matrix estimations in real time, and then recover the original transmitted signals by computing the estimations and the received signals via a demodulation algorithm.

Fig. 6 shows a simplified test setting for the UE antenna element pattern measurements, where the UE is located in a chamber with a measurement antenna connected to the BSE output. In the UE antenna element pattern measurement step, the T/R components of the UE should be kept fixed to a constant value. Only one set of the BSE outputs is used for test signal delivery, so the $S \times U$ transmission can be expressed as

$$\begin{bmatrix} y_1 \\ y_2 \\ \vdots \\ y_U \end{bmatrix} = H(t) * \begin{bmatrix} x_1 \\ 0 \\ \vdots \\ 0 \end{bmatrix}. \tag{10}$$

In this case, the channel matrix $H(t)$ is a static value. The estimation value $H_e(t)$ of $H(t)$ is also static and accessible through the UE reporting, which is defined antenna test function in 3GPP test specification 36.978 [29]. The output power x_1 is known and adjustable, which is set as a constant Q for convenience. Then, the antenna element gains of the UE are

$$\begin{bmatrix} y_1/Q \\ y_2/Q \\ \vdots \\ y_U/Q \end{bmatrix} = H_e(t) * \begin{bmatrix} 1 \\ 0 \\ \vdots \\ 0 \end{bmatrix} \tag{11}$$

where y_u/Q is the gain of the uth antenna element in UE side (with chamber path loss calibrated out). By using the above steps, the gains at all UE orientations of the antenna elements are measured.

After accessing the antenna element patterns through the channel matrix estimation technique, the $S \times U$ matrix $\widetilde{H(t)}$ defined in (6)–(8) is computed via multiplying the measured antenna gain and the channel model, and then integrated into a channel emulator's RF model. This is a step that transfers the S streams to U test signals $(f_1, f_2, \ldots, f_U)$ excited at the channel emulator's U outputs, as shown in Fig. 5.

Third, build the U OTA direct connects between the U channel emulator outputs and the U UE antenna element feedings. So that the signals delivery through the OTA direct connects forms a one-to-one correspondence direct connection, without cross-talking, as if the emulator and UE are directly connected.

B. Implementation of Directly Connected OTA

The implementation of creating the OTA direct connect is illustrated in Fig. 7, where the UE is placed in an anechoic chamber within at least U measurement antennas installed inside. The channel emulator outputs are linked to an RF box that can produce a $U \times U$ static matrix (marked as M

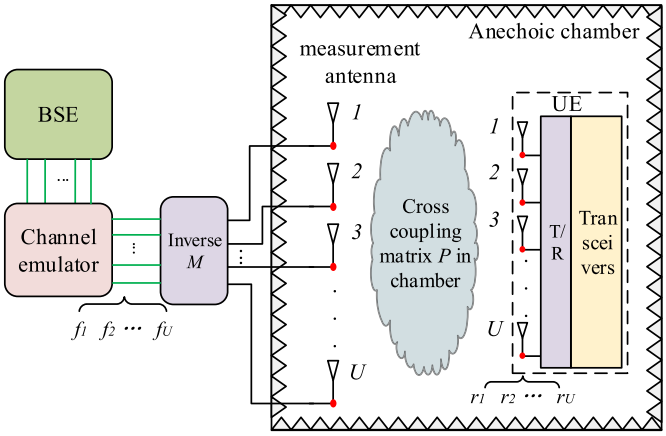

Fig. 7. Test system of the proposed solution.

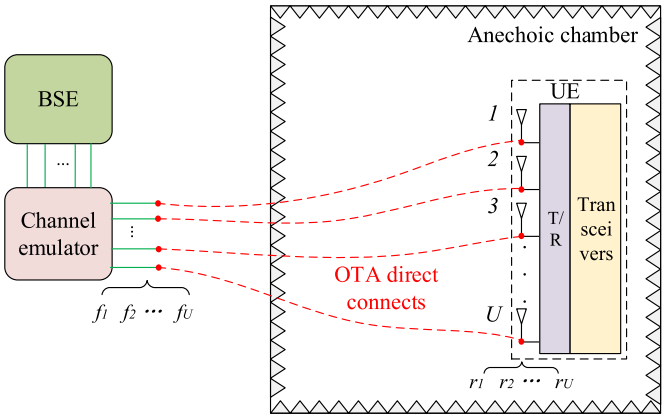

Fig. 8. OTA direct connect diagram.

in the rest of the article). While in chamber, the propagation between the measurement antenna feedings and the UE receiving antenna elements can be expressed as a mathematical matrix (marked as P in the article), which is frequency dependent. In fixed hardware configurations, the factor P is a static value.

Assume that the signals at the UE antenna element feedings are $(r_1, r_2, \ldots, r_U)$ in Fig. 7 that are associated with the signals $(f_1, f_2, \ldots, f_U)$ at the channel emulator outputs as

$$[r_1, r_2, \ldots, r_U]^T = P * M * [f_1, f_2, \ldots, f_U]^T. \quad (12)$$

Setting the matrix M to the inverse of P, we can have that

$$[r_1, r_2, \ldots, r_U]^T = [f_1, f_2, \ldots, f_U]^T. \quad (13)$$

Equation (13) indicates that the channel emulator output signals are delivered into the UE antenna element feedings just like the real cables are used here, which is called the OTA direct connect technique, as shown in Fig. 8. It is worth noting that the OTA direct connect is established based on processing the cross-matrix P in the chamber, which is a factor in terms with the measurement antenna gains, the propagation in chamber, and the UE antenna element gains. That is, a beamforming-independent value, which makes it possible

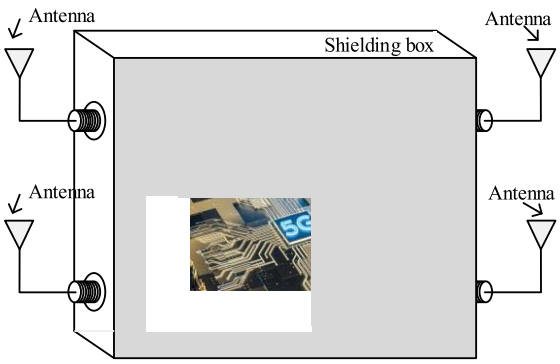

Fig. 9. 5G 4 × 4 MIMO DUT.

for measuring throughput of the adaptive beamforming and antenna-switch UEs in an OTA way.

In short, the test procedure can be divided into three stages: 1) obtain the UE antenna element patterns in the chamber; 2) load the measured UE antenna element patterns and the desired channel model in the emulator for simulations; and 3) build the OTA direct connects between the channel emulator outputs and the UE antenna element feedings and deliver the test signals OTA for throughput testing of UE.

IV. Validation of Proposed Solution

The proposed solution is validated here based on a 4-receiver equipped 5G cellphone, for verifying the feasibility and accuracy. The validation includes three parts: first, the validation of the channel model constructed between S BS antennas and U UE antennas; second, the validation of the isolation of the OTA direct connection; and third, the validation of the rationality and correctness of the final throughput test results. In the OTA direct connection approach, all channel model characteristics are achieved by mathematical calculations in the instrument, which provides higher accuracy compared to the MPAC approach. The channel model validation (including process and results) has been listed in detail in the 3GPP technical report 37.977 [28], the 3GPP test specification 37.544 [4], and the 3GPP test report 38.827 [30], and is not repeated in this article.

As shown in Fig. 8, theoretically, with the inverse matrix applied, the channel emulator output signals are delivered into the UE antenna element feedings just like the real cables are used here. In practice, however, there will always exist cross-couplings between any two OTA direct connect links, mainly caused by the calculation error, circuit coupling, and so on. The ratio of the strength of the transmitted signal to the cross-coupled signal from other ports is the defined isolation of the OTA direct connect. The isolation is specified to be greater than 15 dB during the throughput test, so that the impact of the measurement error due to cross-coupling can be negligible [4].

To verify the accuracy of the proposed method, a specially designed 5G DUT with four transceivers is used. As shown in Fig. 9, the integrated printed circuit board of the DUT (including the four transceivers and all other circuit modules) is sealed

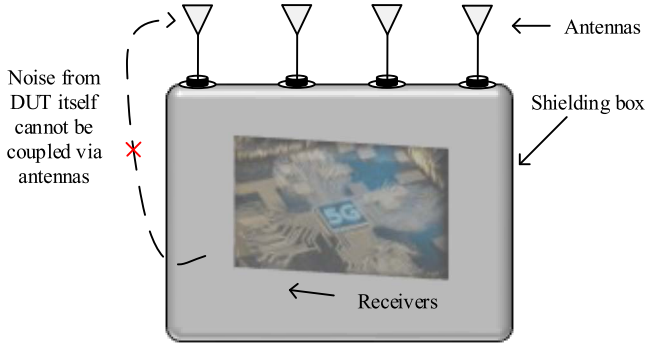

Fig. 10. Noise form the DUT itself cannot be coupled into the receivers via external antennas.

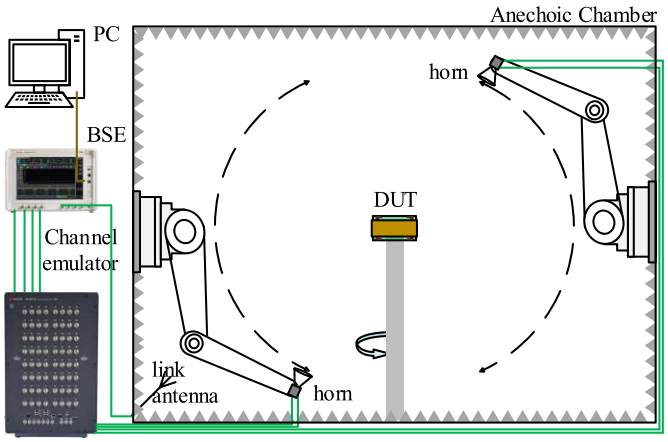

Fig. 11. Test system for conducting the 4 × 4 MIMO OTA measurements of 5G UEs.

in a small shielding box, and its transceiver RF ports are connected to four external antennas through the RF connectors on the shielding box. In this case, the noise radiated by the DUT modules (including the power supply module, crystal oscillator module, camera module, etc.) cannot be captured by the external antenna and then delivered to the receivers, as shown in Fig. 10. As a consequence, the conducted throughput measurements of the DUT and the OTA throughput measurements are theoretically quite consistent for the same protocol configuration. Moreover, the DUT allows four different data streams to be received at a same frequency-time window. The received signal phases are adjustable in order to achieve a simple received beamforming function in UE.

A. Configurations of the Validation System

Fig. 11 shows the system for conducting the 4 × 4 MIMO OTA test based on the proposed scheme, which is consisted of a PC, a BSE, a channel emulator, and an anechoic chamber. The BSE is adopted for producing the four test streams and the T/R functions in BS side, while the channel emulator is utilized for combining the BS antenna element patterns, the multiple path channels, and the DUT antenna element patterns. Moreover, the channel emulator introduced here contains an inside RF box that supports a 4 × 4 matrix loaded. The outputs of the channel emulator are exactly $M * [f_1, f_2, \ldots, f_U]^T$

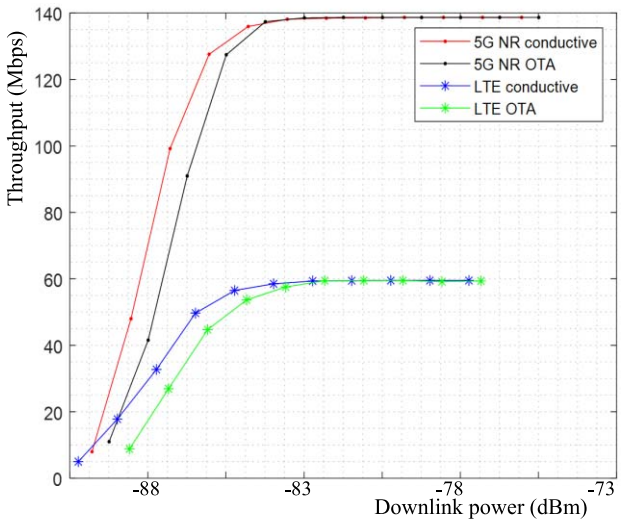

Fig. 12. Comparisons between the conductive measurement results and the OTA measurement results of the 5G UE.

TABLE I
MEASUREMENT PARAMETERS

Parameters		Value
DUT		A cellphone with 4 antennas
Test item		4×4 downlink MIMO throughput
Instruments		Chanel emulator: Propsim F64, BSE: Keysight UXM E7515B
Test protocol		5G new radio (NR) sub-6 GHz non-standalone (NSA) mode
Channel model		CDL-C [27]
Transmission mode		TM3
Configurations for 5G	Max theoretical throughput	138.65Mbps
	Band	41
	BSE configurations	As specified in Section 3.1 in MOSG130715
Configurations for LTE	Max theoretical throughput	59.5Mbps
	Band	3
	BSE configurations	As specified in Section 3.1 and Section 4.6 in MOSG130715

discussed in (12) actually. The chamber contains two dual polarized horn antennas. Each of them is removable along a half ring, in order to measure the 3-D antenna patterns of the DUT and deliver the four test signals to UE antenna feedings. The flexibility of the measurement antenna locations also makes it easier to build the OTA direct connect links with selecting an appreciate condition order related cross coupling matrix in chamber, as mentioned before.

All measurement configurations are listed in Table I. In this article, we follow a clustered delay line (CDL) model defined in 3GPP test report 38.901 [31], for MIMO evaluations, under a consideration that the CDL channel models are standard and recognized in 5G to promote the network performance. The selected CDL channel model is 3-D wave distribution based, and the features as AoA, AoD, Zenith AoD (ZoD), and Zenith AoA (ZoA) are listed in Table II.

TABLE II
FEATURES OF THE SELECTED CDL CHANNEL MODEL

Cluster #	Normalized delay	Power in [dB]	AOD in [°]	AOA in [°]	ZOD in [°]	ZOA in [°]
1	0	-4.4	-46.6	-101	97.2	87.6
2	0.2099	-1.2	-22.8	120	98.6	72.1
3	0.2219	-3.5	-22.8	120	98.6	72.1
4	0.2329	-5.2	-22.8	120	98.6	72.1
5	0.2176	-2.5	-40.7	-127.5	100.6	70.1
6	0.6366	0	0.3	170.4	99.2	75.3
7	0.6448	-2.2	0.3	170.4	99.2	75.3
8	0.6560	-3.9	0.3	170.4	99.2	75.3
9	0.6584	-7.4	73.1	55.4	105.2	67.4
10	0.7935	-7.1	-64.5	66.5	95.3	63.8
11	0.8213	-10.7	80.2	-48.1	106.1	71.4
12	0.9336	-11.1	-97.1	46.9	93.5	60.5
13	1.2285	-5.1	-55.3	68.1	103.7	90.6
14	1.3083	-6.8	-64.3	-68.7	104.2	60.1
15	2.1704	-8.7	-78.5	81.5	93.0	61.0
16	2.7105	-13.2	102.7	30.7	104.2	100.7
17	4.2589	-13.9	99.2	-16.4	94.9	62.3
18	4.6003	-13.9	88.8	3.8	93.1	66.7
19	5.4902	-15.8	-101.9	-13.7	92.2	52.9
20	5.6077	-17.1	92.2	9.7	106.7	61.8
21	6.3065	-16	93.3	5.6	93.0	51.9
22	6.6374	-15.7	106.6	0.7	92.9	61.7
23	7.0427	-21.6	119.5	-21.9	105.2	58
24	8.6523	-22.8	-123.8	33.6	107.8	57

B. Test Results and Analysis

In the validations, the protocol of 5G new radio (NR) nonstandalone (NSA) mode is adopted, which depends on the control plane of an existing long-term evolution (LTE) network for control functions. A total of four sets of throughput test results is generated. The first group is the conductive LTE 4×4 MIMO throughput test results; the second group is the OTA LTE 4×4 MIMO throughput test results; the third group is the conductive 5G NR 4×4 MIMO throughput test results; and the last group is the OTA 5G NR 4×4 MIMO throughput test results. All configurations about the protocol are shown in Table I. The corresponding throughput results are shown in Fig. 12, from which we can get the following remarks.

1) The experiments show that the differences (both on LTE and 5G NR) between the conductive test results and the OTA test results are within 1 dB, which is in good agreement with the theoretical analysis mentioned before. The experiments show that the repeatability of the results is within ± 0.25 dB.
2) Compared to 4G LTE, 5G NR can achieve a significant improvement on throughput rate.
3) All the isolations of the OTA direct connect links are larger than 18 dB, which efficiently meets the requirements of the 3GPP test specifications [4]. It is worth emphasizing that compared with the LTE protocol, 5G MIMO works at a wider bandwidth and the chamber propagation matrix is frequency selective. So for guaranteeing high isolations of the OTA direct connect links, the channel gain flatness at different frequencies in one band of the RF links (mainly determined by the measurement antenna gains, the amplifier gains, and the power loss in the chamber) has to be carefully handled. In this test system, the total gain flatness over one band is within 0.7 dB.

V. CONCLUSION

A new MIMO OTA test solution for 5G UE with adaptive beamforming capability has been proposed through the creation of a directly connected channel between the channel emulator and the DUT, where the true 3-D propagation environment is emulated in the test equipment in order to ensure the DUT working in its normal adaptive beamforming state. The proposed solution and concept are generic, which can be applied to the performance test of different MIMO devices with or without adaptive beamforming. The proposed solution provides both theoretical foundation and test implementation details for the $S \times U$ MIMO beamforming test. To further validate the theoretical analysis and test procedure, a newly developed 4×4 5G MIMO device has been measured in terms of its throughput. For future work, we will propose to apply this scheme to 3-D channel modeling and MIMO OTA testing of huge DUTs and 5G millimeter-wave terminals.

REFERENCES

[1] *Test Plan For Mobile Station Over the Air Performance, Revision 1.0*, CTIA, Washington, DC, USA, Oct. 2001.
[2] "How Many Smartphones are in the World?" Bankmycell. Aug. 2020. [Online]. Available: https://www.bankmycell.com/blog/how-many-phones-are-in-the-world
[3] *Test Plan for Mobile Station Over the Air Performance, Revision 3.8.1*, CTIA, Washington, DC, USA, Oct. 2018.
[4] *User Equipment (UE) Over The Air (OTA) Performance; Conformance Testing*, 3GPP Standard TS 37.544 v14.5.0, 2018.
[5] Y. Qi *et al.*, "5G over-the-air measurement challenges: Overview," *IEEE Trans. Electromagn. Compat.*, vol. 59, no. 6, pp. 1661–1670, Dec. 2017, doi: 10.1109/TEMC.2017.2707471.
[6] J. Li *et al.*, "Temperature effects in OTA MIMO measurement," *IEEE Trans. Instrum. Meas.*, vol. 70, pp. 1–9, 2021, doi: 10.1109/TIM.2020.3014005.
[7] H. L. Van Trees, *Optimum Array Processing: Part IV of Detection, Estimation, and Modulation Theory*. Harlow, U.K.: Prentice-Hall, 2009.
[8] R. A. Monzingo, R. L. Haupt, and T. W. Miller, *Introduction to Adaptive Arrays*. Raleigh, NC, USA: Scitech Publ., 2011.
[9] Y. Sun, L. Zhang, G. Feng, B. Yang, B. Cao, and M. A. Imran, "Blockchain-enabled wireless Internet of Things: Performance analysis and optimal communication node deployment," *IEEE Internet Things J.*, vol. 6, no. 3, pp. 5791–5802, Jun. 2019, doi: 10.1109/JIOT.2019.2905743.
[10] P. Shen, Y. Qi, W. Yu, J. Fan, and F. Li, "OTA measurement for IoT wireless device performance evaluation: Challenges and solutions," *IEEE Internet Things J.*, vol. 6, no. 1, pp. 1223–1237, Feb. 2019, doi: 10.1109/JIOT.2018.2868787.
[11] N. Zhang, P. Yang, J. Ren, D. Chen, L. Yu, and X. Shen, "Synergy of big data and 5G wireless networks: Opportunities, approaches, and challenges," *IEEE Wireless Commun.*, vol. 25, no. 1, pp. 12–18, Feb. 2018, doi: 10.1109/MWC.2018.1700193.
[12] P. Shen, Y. Qi, W. Yu, J. Fan, Z. Yang, and S. Wu, "A decomposition method for MIMO OTA performance evaluation," *IEEE Trans. Veh. Technol.*, vol. 67, no. 9, pp. 8184–8191, Sep. 2018, doi: 10.1109/TVT.2018.2839726.
[13] Y. Jing, H. Kong, and M. Rumney, "MIMO OTA test for a mobile station performance evaluation," *IEEE Instrum. Meas. Mag.*, vol. 19, no. 3, pp. 43–50, Jun. 2016, doi: 10.1109/MIM.2016.7477954.

[14] H. Kong, Z. Wen, Y. Jing, and M. Yau, "Midfield over-the-air test: A new OTA RF performance test method for 5G massive MIMO devices," *IEEE Trans. Microw. Theory Techn.*, vol. 67, no. 7, pp. 2873–2883, Jul. 2019, doi: 10.1109/TMTT.2019.2912369.
[15] M.-T. Dao, V.-A. Nguyen, Y.-T. Im, S.-O. Park, and G. Yoon, "3D polarized channel modeling and performance comparison of MIMO antenna configurations with different polarizations," *IEEE Trans. Antennas Propag.*, vol. 59, no. 7, pp. 2672–2682, Jul. 2011, doi: 10.1109/TAP.2011.2152319.
[16] *Test Plan for 2 × 2 Downlink MIMO and Transmit Diversity Over-the-Air Performance, Revision 1.1*, CTIA, Washington, DC, USA, Aug. 2016.
[17] W. Yu, Y. Qi, K. Liu, Y. Xu, and J. Fan, "Radiated two-stage method for LTE MIMO user equipment performance evaluation," *IEEE Trans. Electromagn. Compat.*, vol. 56, no. 6, pp. 1691–1696, Dec. 2014, doi: 10.1109/TEMC.2014.2320779.
[18] W. Fan, P. Kyösti, J. Ø. Nielsen, and G. F. Pedersen, "Wideband MIMO channel capacity analysis in multiprobe anechoic chamber setups," *IEEE Trans. Veh. Technol.*, vol. 65, no. 5, pp. 2861–2871, May 2016, doi: 10.1109/TVT.2015.2435813.
[19] W. Fan, P. Kyösti, L. Hentilä, and G. F. Pedersen, "MIMO terminal performance evaluation with a novel wireless cable method," *IEEE Trans. Antennas Propag.*, vol. 65, no. 9, pp. 4803–4814, Sep. 2017, doi: 10.1109/TAP.2017.2723260.
[20] J. O. Nielsen, W. Fan, P. C. F. Eggers, and G. F. Pedersen, "A channel sounder for massive MIMO and MmWave channels," *IEEE Commun. Mag.*, vol. 56, no. 12, pp. 67–73, Dec. 2018, doi: 10.1109/MCOM.2018.1800199.
[21] "Spatial channel model for multiple input multiple output (MIMO) simulations," 3GPP, Sophia Antipolis, France, 3GPP Rep. TR 25.996 V13.0.0, Dec. 2015.
[22] W. Fan, F. Zhang, and Z. Wang, "Over-the-air testing of 5G communication systems: Validation of the test environment in simple-sectored multiprobe anechoic chamber setups," *IEEE Antennas Propag. Mag.*, vol. 63, no. 1, pp. 40–50, Feb. 2021, doi: 10.1109/MAP.2019.2943305.
[23] W. Fan *et al.*, "A step toward 5G in 2020: Low-cost OTA performance evaluation of massive MIMO base stations," *IEEE Antennas Propag. Mag.*, vol. 59, no. 1, pp. 38–47, Feb. 2017, doi: 10.1109/MAP.2016.2630020.
[24] L. Xin, Y. Li, S. Zhe, and X. Zhang, "On over-the-air testing for devices with directional antennas," *IEEE Access*, vol. 8, pp. 121821–121832, 2020, doi: 10.1109/ACCESS.2020.3007450.
[25] M. Á. García-Fernández and D. A. Sánchez-Hernández, "Beamforming evaluation of 5G user equipment through novel key performance indicators," *Electronics*, vol. 10, p. 1319, May 2021.
[26] "Technical specification group radio access network; NR; Study on test methods," 3GPP, Sophia Antipolis, France, 3GPP Rep. TR 38.810, Dec. 2018.
[27] *NR; User Equipment (UE) Radio Transmission and Reception*, 3GPP Standard TS 38.101, Jun. 2017.
[28] "Verification of radiated multi-antenna reception performance of user equipment (UE), revision 15.0.0," 3GPP, Sophia Antipolis, France, 3GPP Rep. TR 37.977, Sep. 2018.
[29] *User Equipment (UE) Antenna Test Function Definition for Two-Stage Multiple Input Multiple Output (MIMO) Over The Air (OTA) Test Method, V13.2.0*, 3GPP Standard TS 36.978, 2017.
[30] "Study on radiated metrics and test methodology for the verification of multi-antenna reception performance of NR user equipment (UE), v16.0.0," 3GPP, Sophia Antipolis, France, 3GPP Rep. TR 38.827, 2020.
[31] "Study on channel model for frequencies from 0.5 to 100 GHz, v16.1.0," 3GPP, Sophia Antipolis, France, 3GPP Rep. TR 38.901, 2019.

Penghui Shen (Student Member, IEEE) received the B.S., M.S., and Ph.D. degrees in electronic information and technology from Hunan University, Changsha, China, in 2013, 2016, and 2020, respectively.

He is currently a Postdoctoral Researcher with the Department of Mathematics and Theory, Peng cheng Laboratory, Shenzhen, China. His research interests include SISO, MIMO, and 5G array measurements for wireless devices, EMC, and antenna design.

Yihong Qi (Senior Member, IEEE) received the B.S. degree in electronics from the National University of Defense Technologies, Changsha, China, in 1982, the M.S. degree in electronics from the Chinese Academy of Space Technology, Beijing, China, in 1985, and the Ph.D. degree in electronics from Xidian University, Xi'an, China, in 1989.

From 1989 to 1993, he was a Postdoctoral Fellow and then an Associate Professor with Southeast University, Nanjing, China. From 1993 to 1995, he was a Postdoctoral Researcher with McMaster University, Hamilton, ON, Canada. From 1995 to 2010, he was with Research in Motion (Blackberry), Waterloo, ON, Canada, where he was the Director of Advanced Electromagnetic Research. He is currently a Scientist with Peng Cheng Laboratory, Shenzhen, China, and the President and the Chief Scientist with General Test Systems, Inc., Shenzhen; he founded DBJay, Zhuhai, China, in 2011. He is also an Adjunct Professor with the EMC Laboratory, Missouri University of Science and Technology, Rolla, MO, USA; Western University, London, ON, Canada; and Hunan University, Changsha, and an Honorary Professor with Southwest Jiaotong University, Chengdu, China. He is an inventor of more than 450 published and pending patents.

Dr. Qi has received the IEEE EMC Society Technical Achievement Award in August 2017. He was a Distinguished Lecturer of the IEEE EMC Society for 2014 and 2015, and the Founding Chairman of the IEEE EMC TC-12. He is a Fellow of the Canadian Academy of Engineering and National Academy of Inventors.

Wei Yu (Senior Member, IEEE) received the B.S. degree in electrical engineering from Xi'an Jiaotong University, Xi'an, China, in 1991, the M.S. degree in electrical engineering from China Academy of Space Technology, Beijing, China, in 1994, and the Ph.D. degree in electrical engineering from Xidian University, Xi'an, in 2000.

From 2001 to 2003, he was a Postdoctoral Fellow with the University of Waterloo, Waterloo, ON, Canada. He was a CTO with Sunway Communications Ltd., Shenzhen, China, from 2008 to 2012. He founded Antenovation Electronics Inc., Shenzhen, in 2004, and co-founded General Test Systems Inc., Shenzhen, in 2012. He is currently with General Test Systems, Shenzhen, as a CEO. He has invented 91 published and pending patents. His current research interests include signal processing and mobile device test system.

Fuhai Li (Member, IEEE) received the B.S. and M.S. degrees in instrument science and technology from Hunan University, Changsha, China, from 1982 to 1988.

He is a Professor with Hunan University. He had published more than 30 papers in the national core journals and involved the compiling of university teaching materials.

Prof. Li had several science and technology progress awards during his tenure. His students had lots of awards in kinds of national competitions under his leadership.

Xianbin Wang (Fellow, IEEE) received the Ph.D. degree in electrical and computer engineering from the National University of Singapore, Singapore, in 2001.

He is a Professor and the Tier-1 Canada Research Chair with Western University, London, ON, Canada. Prior to joining Western University, he was with Communications Research Centre Canada (CRC), Ottawa, ON, Canada, as a Research Scientist/Senior Research Scientist from July 2002 and December 2007. From January 2001 to July 2002, he was a System Designer with STMicroelectronics, Geneva, Switzerland. He has over 450 highly cited journal and conference papers, in addition to 30 granted and pending patents and several standard contributions. His current research interests include 5G/6G technologies, Internet of Things, communications security, machine learning, and intelligent communications.

Prof. Wang has received many awards and recognitions, including the Canada Research Chair, the CRC President's Excellence Award, the Canadian Federal Government Public Service Award, the Ontario Early Researcher Award, and six IEEE best paper awards. He has been nominated as an IEEE Distinguished Lecturer several times during the last ten years. He currently serves/has served as an editor-in-chief, an associate editor-in-chief, and an editor/associate editor for over ten journals. He was involved in many IEEE conferences, including GLOBECOM, ICC, VTC, PIMRC, WCNC, CCECE, and CWIT, in different roles, such as the General Chair, the Symposium Chair, the Tutorial Instructor, the Track Chair, the Session Chair, the TPC Co-Chair, and a Keynote Speaker. He is currently serving as the Chair of IEEE London Section and the Chair of ComSoc Signal Processing and Computing for Communications Technical Committee. He is a Fellow of the Canadian Academy of Engineering and the Engineering Institute of Canada and an IEEE Distinguished Lecturer.

Xuemin (Sherman) Shen (Fellow, IEEE) received the Ph.D. degree in electrical engineering from Rutgers University, New Brunswick, NJ, USA, in 1990.

He is currently a University Professor with the Department of Electrical and Computer Engineering, University of Waterloo, Waterloo, ON, Canada. His research focuses on network resource management, wireless network security, Internet of Things, 5G and beyond, and vehicular ad hoc and sensor networks.

Prof. Shen received the R.A. Fessenden Award in 2019 from IEEE, Canada, the Award of Merit from the Federation of Chinese Canadian Professionals (Ontario) presents in 2019, the James Evans Avant Garde Award in 2018 from the IEEE Vehicular Technology Society, the Joseph LoCicero Award in 2015 and the Education Award in 2017 from the IEEE Communications Society, and the Technical Recognition Award from Wireless Communications Technical Committee in 2019 and AHSN Technical Committee in 2013. He has also received the Excellent Graduate Supervision Award in 2006 from the University of Waterloo and the Premier's Research Excellence Award in 2003 from the Province of Ontario, Canada. He served as the Technical Program Committee Chair/Co-Chair for IEEE Globecom'16, IEEE Infocom'14, IEEE VTC'10 Fall, and IEEE Globecom'07, the Symposia Chair for IEEE ICC'10, and the Chair for the IEEE Communications Society Technical Committee on Wireless Communications. He is the Elected IEEE Communications Society Vice President for Technical and Educational Activities, the Vice President for Publications, the Member-at-Large on the Board of Governors, the Chair of the Distinguished Lecturer Selection Committee, and the member of the IEEE Fellow Selection Committee. He was/is the Editor-in-Chief of the IEEE INTERNET OF THINGS JOURNAL, IEEE NETWORK, *IET Communications*, and *Peer-to-Peer Networking and Applications*. He is a registered Professional Engineer of Ontario, Canada, a Fellow of the Engineering Institute of Canada, the Canadian Academy of Engineering, and the Royal Society of Canada, a Foreign Fellow of the Chinese Academy of Engineering, and a Distinguished Lecturer of the IEEE Vehicular Technology Society and Communications Society.